

KERR ROTATION AND MAGNETIC CIRCULAR DICHROISM SPECTRA OF FERROMAGNETIC InMnSb AND InMnAs

Andreas Winter¹, Harald Pascher¹, Michael Hofmayer², Heinz Krenn², Tomasz Wojtowicz^{3,4}, Xinyu Liu³ and Jacek K. Furdyna³

¹Experimentalphysik I, Universität Bayreuth, D-95440 Bayreuth, Germany

²Institut für Experimentalphysik, Karl-Franzens-Universität, A-8010 Graz, Austria

³Department of Physics, University of Notre Dame, Notre Dame, Indiana 46556, USA

⁴Institute of Physics, Polish Academy of Sciences, 02-668 Warsaw, Poland

Received: February 03, 2008

Abstract. Magneto-optical Kerr rotation and magnetic circular dichroism (MCD) have been measured in thin epitaxial layers of the narrow gap ferromagnetic semiconductors InMnSb and InMnAs grown by low-temperature molecular beam epitaxy. The measurements were carried out in the wavelength range from 400 to 7000 nm. The wavelength dependence of Kerr rotation and MCD were modelled using the same set of parameters. To calculate the Landau level energies for the above systems we have used a $\vec{k} \cdot \vec{p}$ -model developed by Trebin *et al.* [1,2] combined with an exchange matrix, as described by Rigaux [3]. Taking into account transition energies corresponding to the selection rules for right and left circularly polarized light enabled us to calculate both Kerr rotation and MCD using procedures described by Lang *et al.* [4]. The fits yield values for the exchange parameters $N_0\alpha$ and $N_0\beta$.

1. INTRODUCTION

The discovery of ferromagnetism in the dilute magnetic semiconductor GaMnAs [5] has promoted intense research on the exchange interaction mechanisms in III-V semiconductors alloyed with Mn [6]. In contrast to the widely investigated system GaMnAs, in ferromagnetic InMnSb [7] and InMnAs [8] the large effective g -factor of the narrow gap host material has to be considered in band structure models for these alloys in an external magnetic field. Thin layers of InMnSb and InMnAs are investigated by polar magneto-optical Kerr effect (MOKE) and reflectance magnetic-circular dichroism (MCD). The model described below was fitted simultaneously to MOKE and MCD spectra, yielding consistent sets of band and exchange parameters for both materials.

2. DILUTED MAGNETIC SEMICONDUCTORS

By alloying a semiconductor with an element which exhibits a magnetic moment, an exchange interaction between the localized magnetic moments and the free carriers occurs, which strongly affects the band structure of the semiconducting material. These so called diluted magnetic semiconductors (DMSs) have interesting properties allowing possible applications, such as magnetic memories completely fabricated of semiconductors. Concerning the magnetic properties one finds – depending on concentration x of the magnetic ions and the free carrier density – paramagnetism, antiferromagnetism, spin-glass and ferromagnetism [11,5]. The spins $S=5/2$ (in the case of Mn^{2+}) orient themselves along the magnetic field direction. The mean value

Corresponding author: Andreas Winter, e-mail: andreas.winter@uni-bayreuth.de

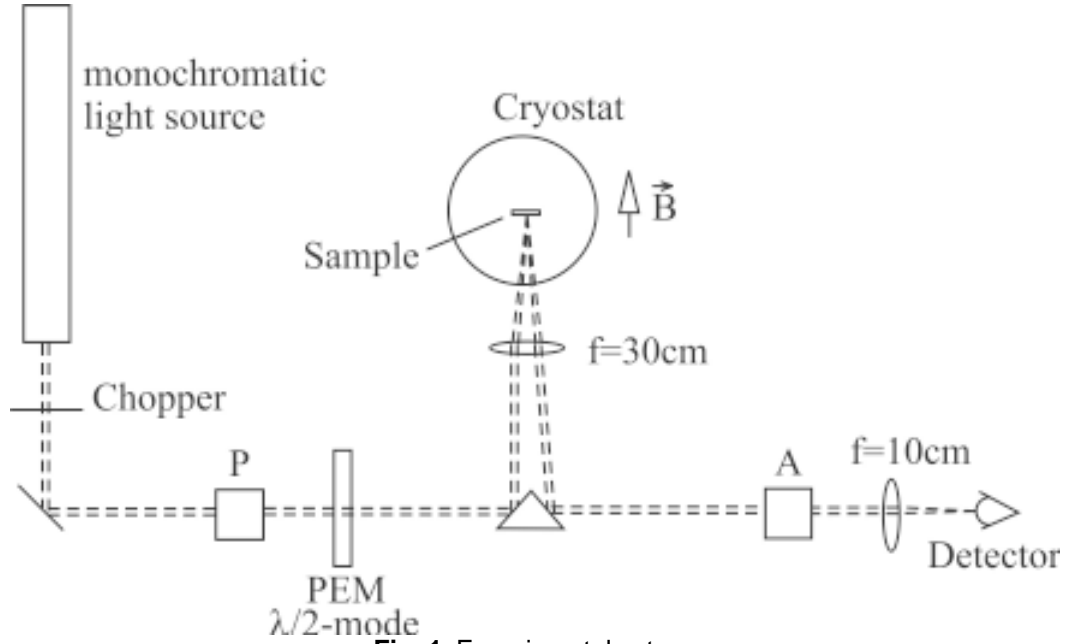


Fig. 1. Experimental setup.

of the isolated spin can be described by a Brillouin-function

$$\langle S_z \rangle = \frac{5}{2} \cdot B_{5/2} \left(\frac{g\mu_B B}{k_B T} \right). \quad (1)$$

The magnetization is

$$M = xN_0 g\mu_B \langle S_z \rangle, \quad (2)$$

where N_0 is the density of cations, μ_B is the Bohr magneton and $g=2$.

InMnSb [7] and InMnAs [8] are examples of III-V-based ferromagnetic semiconductors. In their case the Mn^{2+} -ions partly replace the element from the third group and therefore act as acceptors. This results in a highly p-doped semiconductor. The hole gas couples the spins of the Mn-ions, which can then lead to long range ferromagnetic order. A very well studied example is the wide gap semiconductor GaMnAs, which becomes ferromagnetic for Mn-concentration higher than 1%. Curie temperatures well above liquid nitrogen temperature have been obtained for this alloy.

The present investigation deals with InMnSb and InMnAs. These materials are interesting because they exhibit a large lattice constant and a small gap, resulting in small effective masses and high carrier mobility.

3. EXPERIMENTAL SETUP

For the investigation of samples exhibiting semi-conducting and magnetic properties at the same time, magneto-optical effects are very well suited. One of these effects is the so-called magneto-optical Kerr effect (MOKE), i.e., the rotation of the plane of polarization of linearly polarized light reflected from the surface of a magnetized sample. The case when the k -vector of the incident light is parallel to the magnetic field is referred to as the polar MOKE.

In magnetic semiconductors the spin splitting of the energy bands is strongly influenced by the magnetization and the exchange interaction between localized magnetic moments and band carriers. The difference of the splitting in the valence and the conduction band manifests itself in different refractive indices for left and right circularly polarized components of the linearly polarized incident light beam (which we will refer to as σ^+ and σ^- polarizations, respectively). When the light beam is reflected from the sample surface, the two circularly polarized components then suffer different phase shifts. The two reflected components recombine to form a linearly polarized beam that is rotated with respect to the initial polarization due to their phase difference.

This can be described by Fresnel's formula for reflection of the electric field E at the interface be-

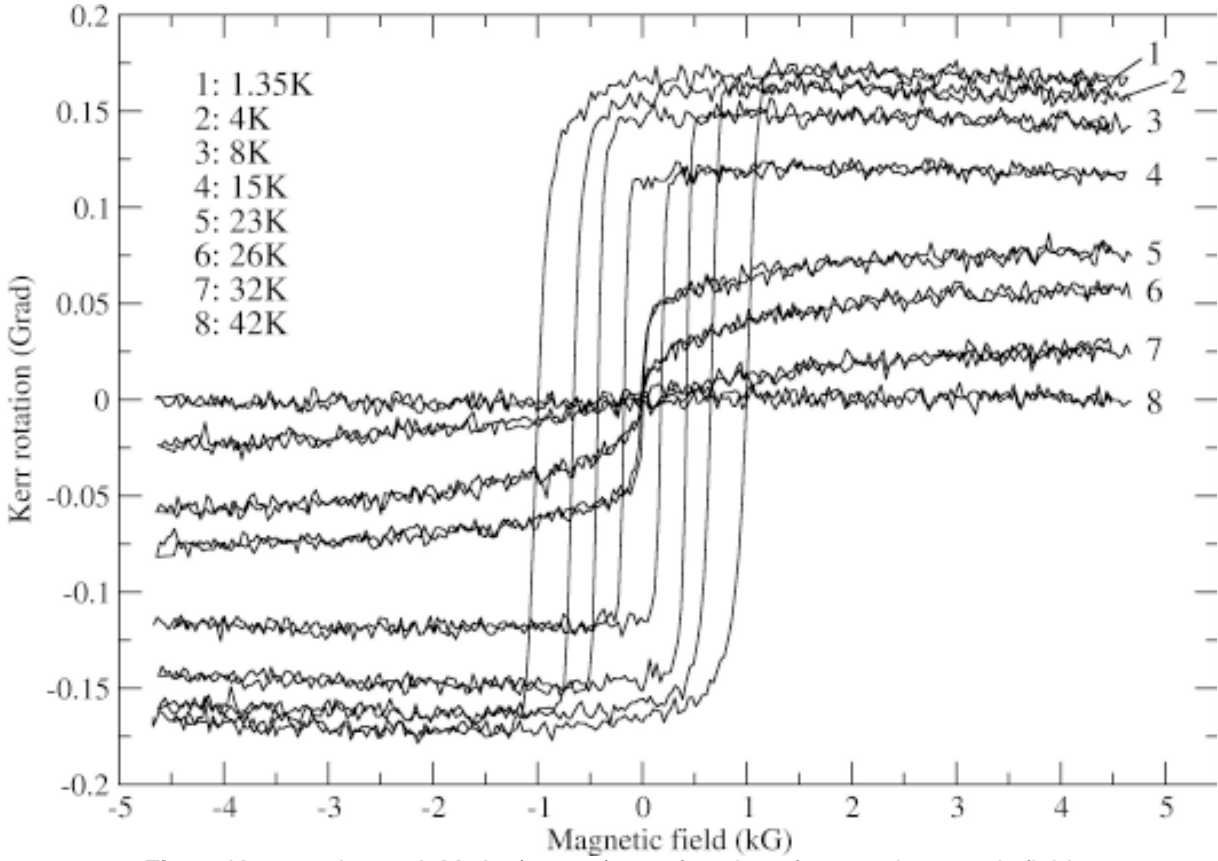


Fig. 2. Kerr rotation on InMnAs ($x=0.08$) as a function of external magnetic field.

tween a medium with refractive index 1 (air) and a medium with complex refractive indices $\tilde{n}_{\pm} = n_{\pm} - i\chi_{\pm}$ (the diluted magnetic semiconductor), where the + and - subscripts correspond to the σ^+ and σ^- polarizations, respectively:

$$E_{refl} = \tilde{r}_{\pm} E_0 = \frac{1 - \tilde{n}_{\pm}}{1 + \tilde{n}_{\pm}} E_0, \quad (3)$$

where $\tilde{r}_{\pm} = r_{\pm} \exp(i\phi_{\pm})$ is the complex reflection coefficient. From Eq. (3) we directly obtain:

$$\phi_{\pm} = \arctan\left(\frac{2\chi_{\pm}}{1 - n_{\pm}^2 - \chi_{\pm}^2}\right). \quad (4)$$

The Kerr rotation is then calculated to be

$$\theta_{Kerr} = \frac{1}{2}(\phi_{-} - \phi_{+}); \quad (5)$$

and the difference in the reflectivities of the left and right circularly polarized light is the MCD, defined as:

$$MCD = \left(\frac{r_{+}^2 - r_{-}^2}{r_{+}^2 + r_{-}^2}\right). \quad (6)$$

Fig. 1 shows a schematic diagram of the experimental setup used for polar Kerr effect measurements. A halogen lamp or globar together with a grating spectrometer or a CO-laser were used as monochromatic light sources. Behind the first polarizer P the light is polarized vertically. After passing the photoelastic modulator (PEM) the polarization vector of the light is switched from vertical to horizontal polarization with a frequency of about 50 kHz. The light reflected from the sample is detected after passing through the analyzer A, oriented 45° away from the vertical direction. At $B=0$ the projections of the electric field orientations behind the PEM on the direction of the analyzer are equal. A lock-in amplifier that obtains its reference from the modulator and the signal from the detector measures the difference between the two projections (which, as noted, is zero at $B=0$). If the sample rotates the plane of polarization, the differ-

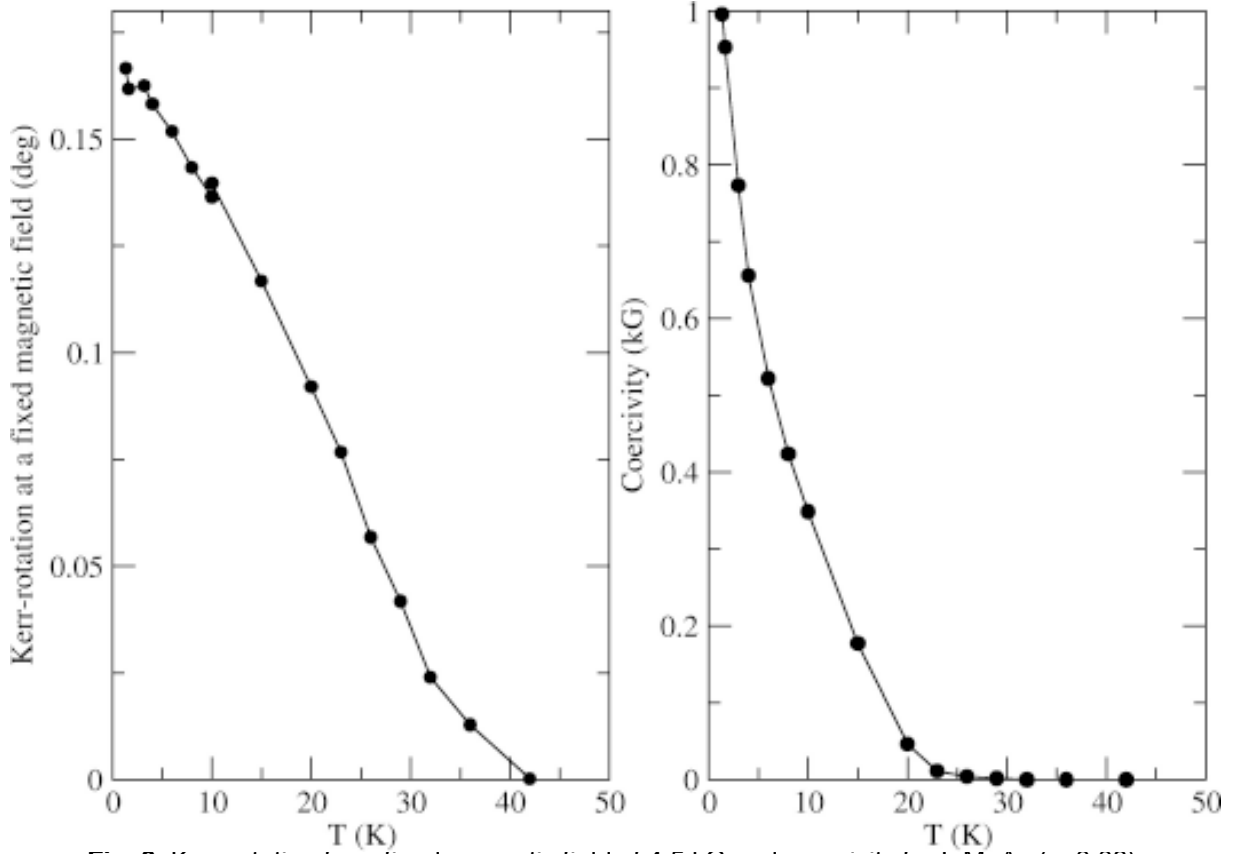


Fig. 3. Kerr rotation for a fixed magnetic field of 4.5 kG and coercivity for InMnAs ($x=0.08$).

ence between the two projections no longer vanishes and is detected by the lock-in amplifier. We refer to this signal as “DLI” (difference lock-in). A second lock-in amplifier, receiving its reference from the chopper, measures the overall intensity “SLI” (sum lock-in). From both signals the rotation angle Θ_{Kerr} of the polarization of the reflected light can be calculated by:

$$\Theta_{Kerr} = \frac{1}{2} \arcsin \left(\frac{\frac{DLI}{SLI}}{\frac{I_2}{8} - \frac{I_1}{2\pi} \cdot \frac{DLI}{SLI}} \right). \quad (7)$$

The constants I_1 and I_2 can be calculated numerically from the working principle of a lock-in amplifier. However, even small misalignments of the directions of the polarizers affect these constants. Therefore, in order to improve the experimental accuracy, the constants were determined from a calibration measurement.

The use of a differential method makes this experimental setup highly sensitive, enabling us to

resolve rotations of polarization of the reflected light with an accuracy of up to 0.002 degree. For the measurement of MCD, the PEM is used in the $\lambda/4$ mode and the analyzer behind the sample is removed. Then the DLI lock-in amplifier measures the difference of the reflected intensities R_+ and R_- of the σ^+ and σ^- polarizations, and the SLI lock-in amplifier measures their sum. From both quantities the MCD can then be readily obtained.

These experiments yield the magnetic field dependence of the magnetization if measurements are done at a fixed wavelength; and at a fixed magnetic field the wavelength dependence (the spectra) of the magneto-optical effects can be recorded.

4. MODEL CALCULATION OF KERR-ROTATION AND MCD IN NARROW GAP SEMICONDUCTORS

As mentioned above, the MOKE and MCD magneto-optical effects depend on the complex refractive indices \tilde{n} for the σ^+ and σ^- polarizations, and thus on the corresponding dielectric functions

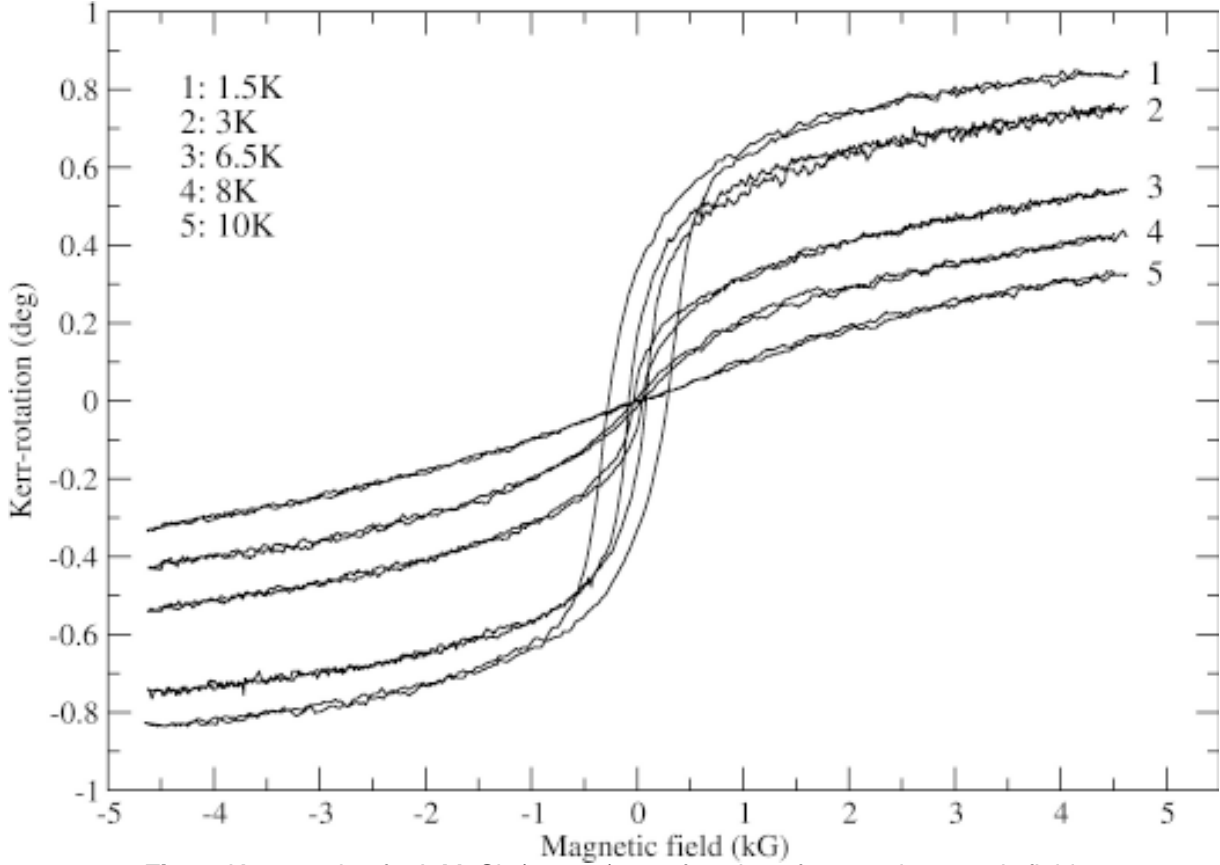


Fig. 4. Kerr rotation for InMnSb ($x=0.02$) as a function of external magnetic field.

$\varepsilon = \tilde{n}^2$. In the frequency range, where our experiments were performed, one has to consider magneto-optical interband transitions between states $|i\rangle$ and $|j\rangle$ at different wavevectors k_z (magnetic field B in z -direction). According to Kim *et al.* [10] the dielectric function is calculated by:

$$\varepsilon_{\pm}(\omega) = \varepsilon_{\infty} - \frac{8\pi\hbar^2 e^2}{m_0 \varepsilon_0} \sum_{i,j,k} \frac{f_{ijk}^2}{(\omega_{ijk}^{\pm})^2} \left(\frac{1}{\omega - \omega_{ijk}^{\pm} + i\Gamma} - \frac{1}{\omega + \omega_{ijk}^{\pm} + i\Gamma} \right). \quad (7)$$

Here $\hbar\omega_{ijk}^{\pm}$ is the transition energy between valence- and conduction band states $|i\rangle$ and $|j\rangle$ at the wavevector $k=k_z$ allowed for σ^+ respectively σ^- polarized light; and f_{ijk} is the corresponding oscillator strength.

The difference of the refractive indices for σ^+ and σ^- light determining Θ_{Kerr} (see Eq. (5)) mainly depends on the difference of the spin splittings of

the valence and the conduction band. For the g -factor of electrons in a DMS one can write:

$$g^* = g_0^* \mu_B B + \frac{\alpha M}{\mu_B B}. \quad (8)$$

(with an analogous expression for the valence band, using exchange constant β instead of α). Here g_0^* is the g -factor of hypothetical material without magnetic ions, and α exchange constant for the conduction band.

In wide gap semiconductors the first term in Eq. (8) usually is much smaller than the second, and can be neglected (e.g., for GaAs: $|g^*|=0.44$). This is no longer true, however, for narrow gap materials with their huge g -factors (for InSb: $|g^*|=50$). Therefore in InMnSb and InMnAs the electronic states have to be obtained by including the exchange interaction in a $\vec{k} \cdot \vec{p}$ band structure model. We use a model calculation described by Trebin *et al.* [1,2].

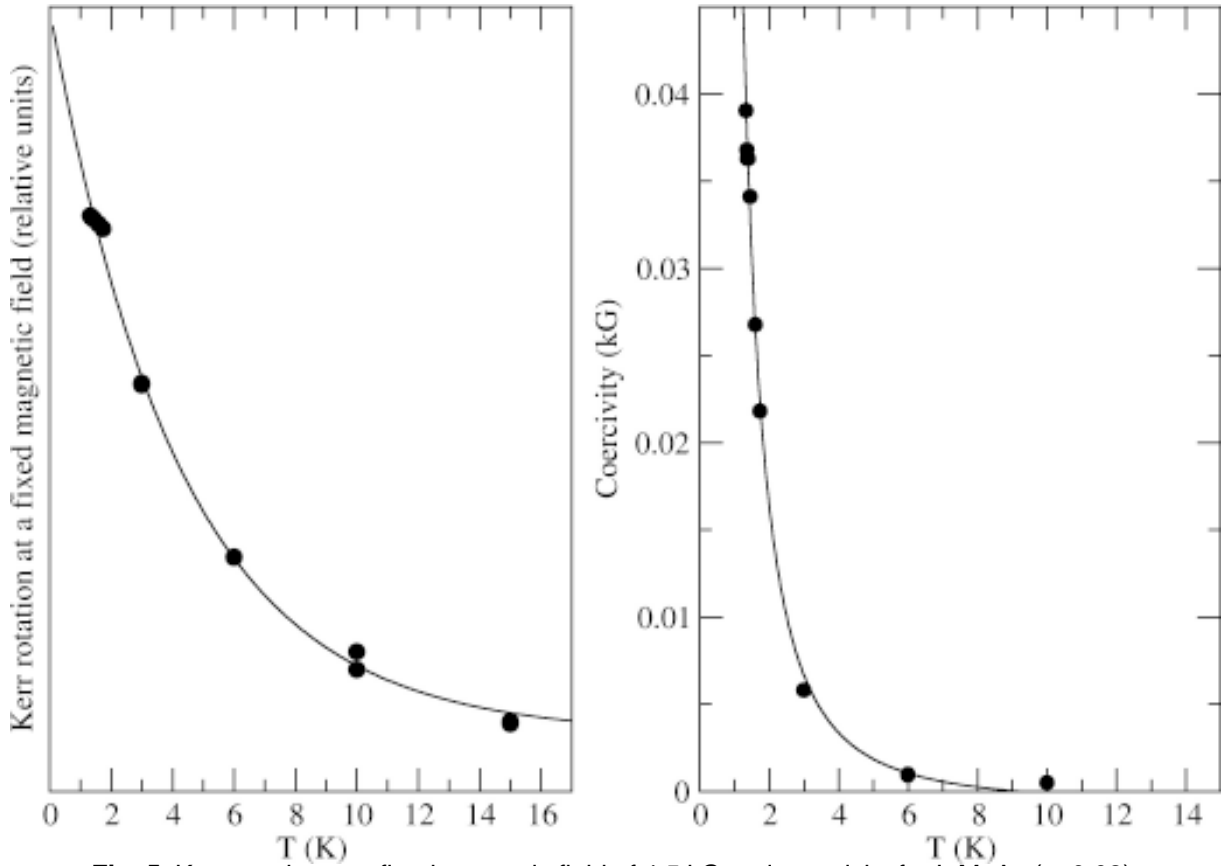


Fig. 5. Kerr rotation at a fixed magnetic field of 4.5 kG and coercivity for InMnAs ($x=0.02$).

For each k -value two large matrices have to be diagonalized. Each matrix contains 4×4 blocks for each Landau quantum number, describing the $\vec{k} \cdot \vec{p}$ interaction of the conduction band, the spin orbit split-off band, and the two valence bands for light and heavy holes. To account for the exchange interaction, the Hamiltonian is supplemented by additional 4×4 blocks for each Landau level containing the exchange constants. These are determined by a least squares fit to our measurements. This procedure yields energies $\hbar\omega_{ijk}^{\pm}$ and relative oscillator strengths f_{ijk} necessary for the calculation of the dielectric functions via to Eq. (7).

5. RESULTS

By using a fixed wavelength and sweeping the external magnetic field it is possible to record hysteresis loops of ferromagnetic semiconductors at different temperatures (see Fig. 2). From such recordings the coercivity as a function of temperature is obtained, yielding the Curie temperature (see

Fig. 3). Fig. 3 reveals the Curie temperature of our InMnAs-sample to be 30K.

In contrast to InMnAs, in InMnSb the magnetization still increases for magnetic fields above the field where the magnetization is the same for sweep up and sweep down (about 1 kG in Fig. 4). This demonstrates that there is always a noticeable paramagnetic contribution present. In this case the coercivity versus temperature indicates a Curie temperature of 9K (see Fig. 5).

To check the theoretical model we measured the Kerr- and MCD-spectra of InSb at fixed magnetic fields. Fig. 6 demonstrates that there is rather satisfactory agreement between experiment and model calculations. It should be noted that no free fitting parameters were used except the damping constant G and a normalization constant.

When sweeping the magnetic field at a fixed photon energy above the energy gap, one observes oscillations in the dependence of Θ_{Kerr} on B , which according to our calculations correspond to specific transitions. Specifically, at a magnetic field

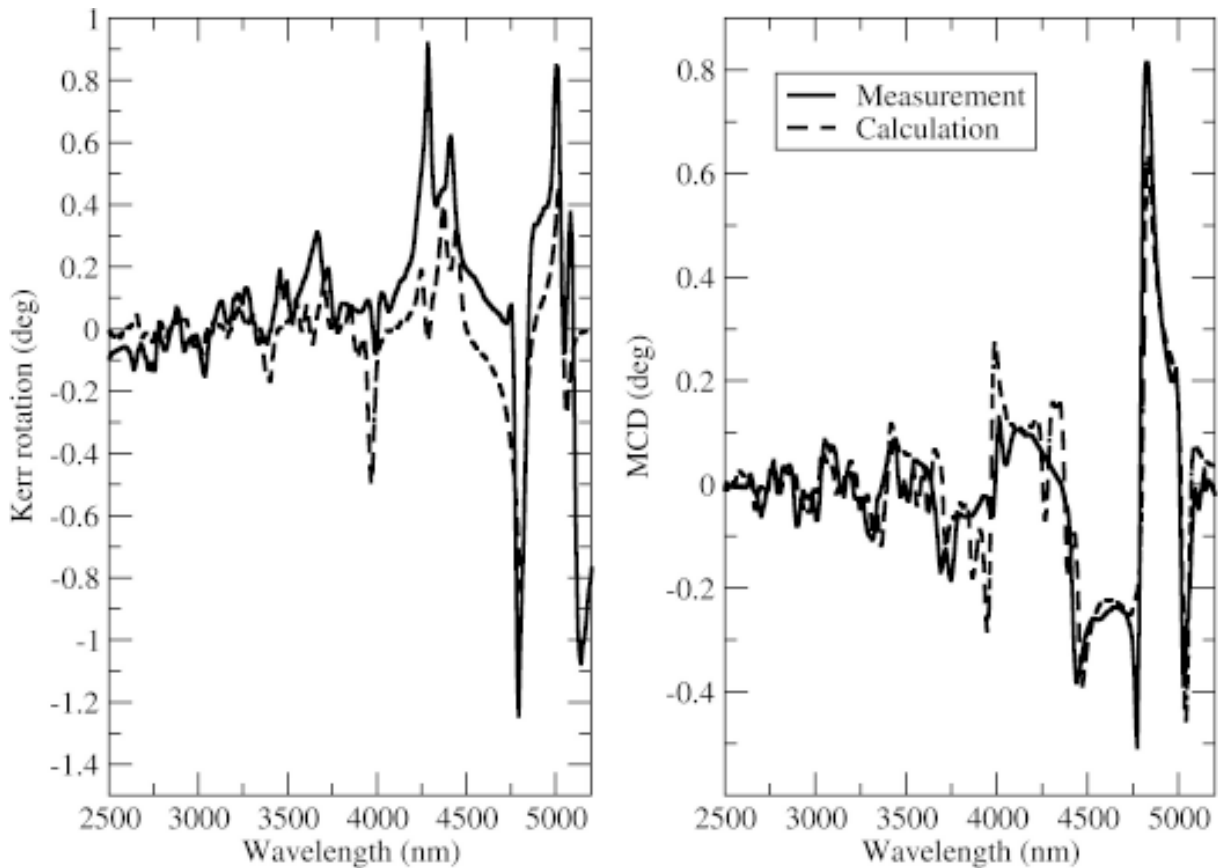


Fig. 6. Measured and calculated Kerr rotation- and MCD-spectra of pure InSb at $B=45.7$ kG and temperature $T=1.6$ K.

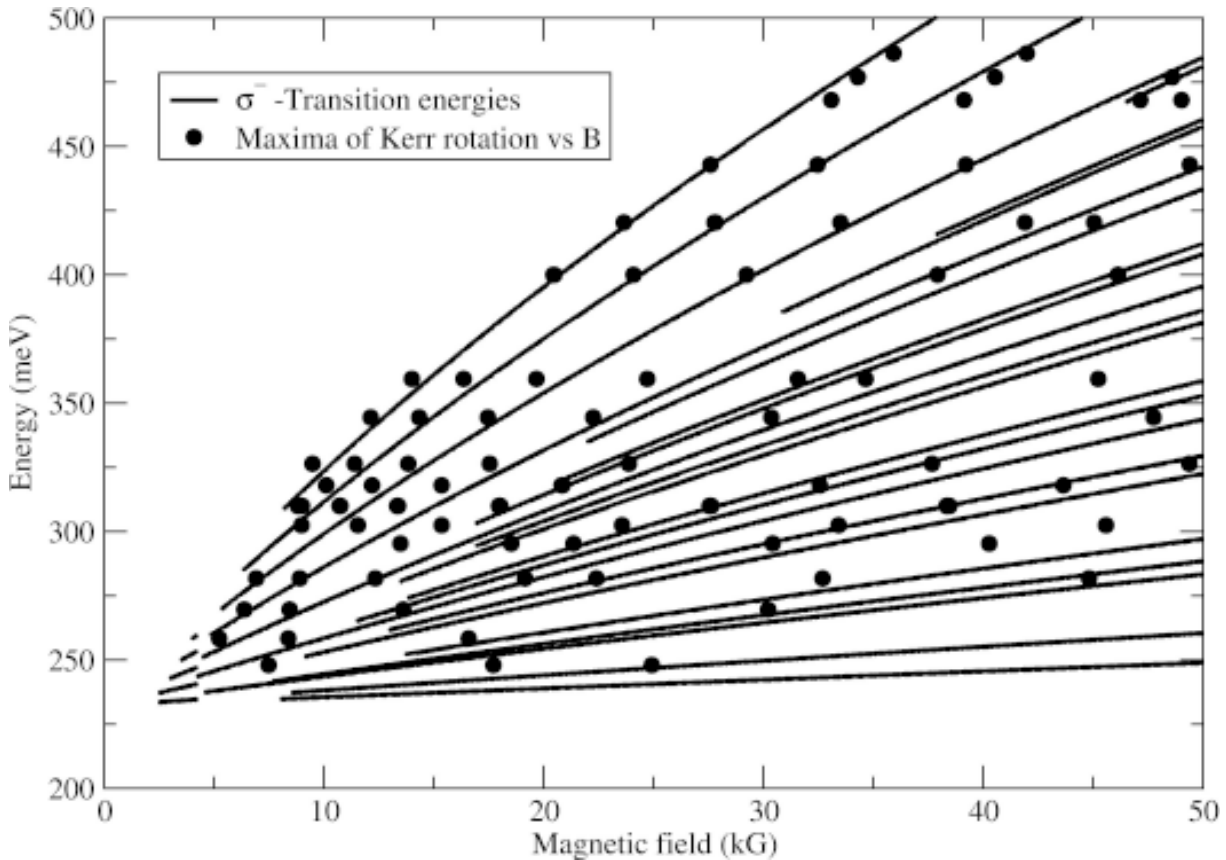


Fig. 7. Calculated and measured σ^- -transition-energies versus the magnetic field in pure InSb, temperature $T=1.6$ K.

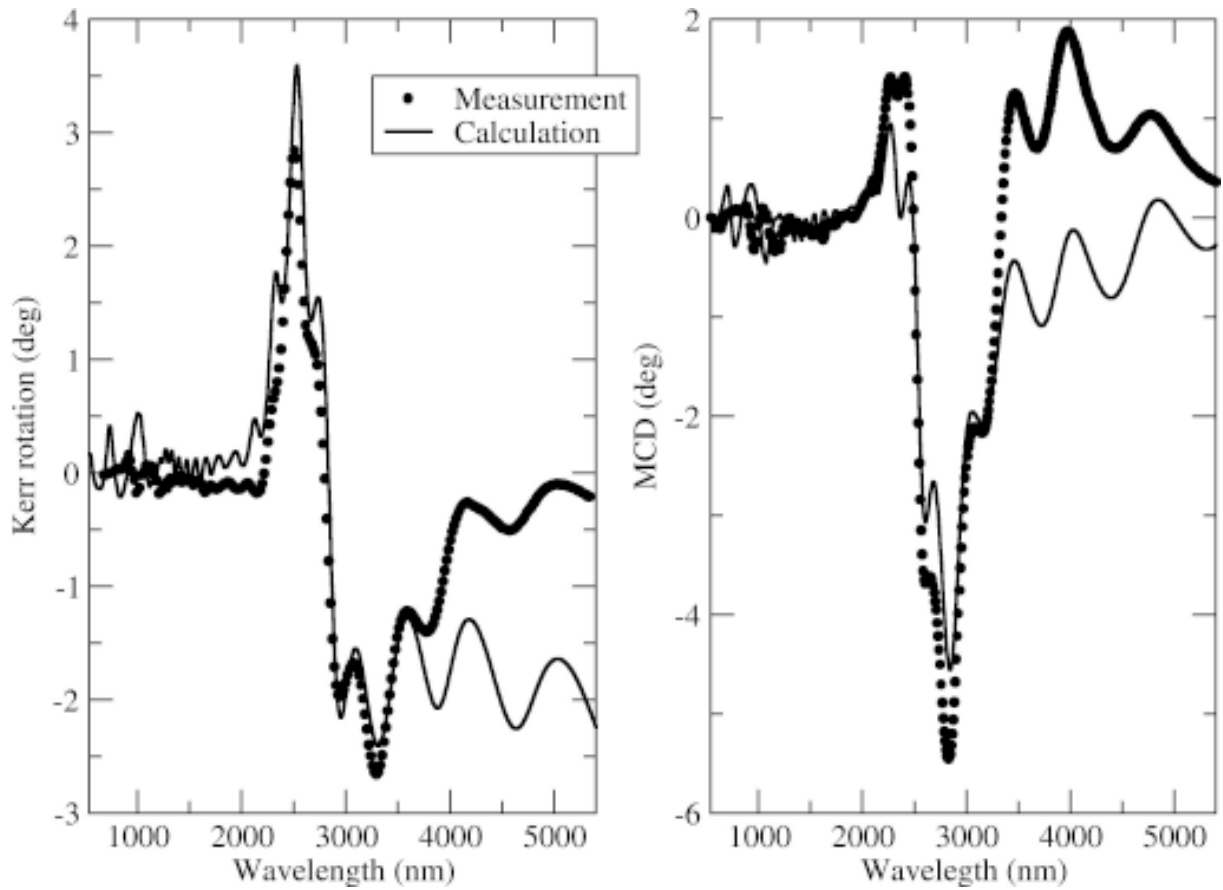


Fig. 8. Kerr and MCD spectra for InMnSb ($x=0.015$) at a fixed magnetic field of 4.5 kG and temperature $T=1.6$ K.

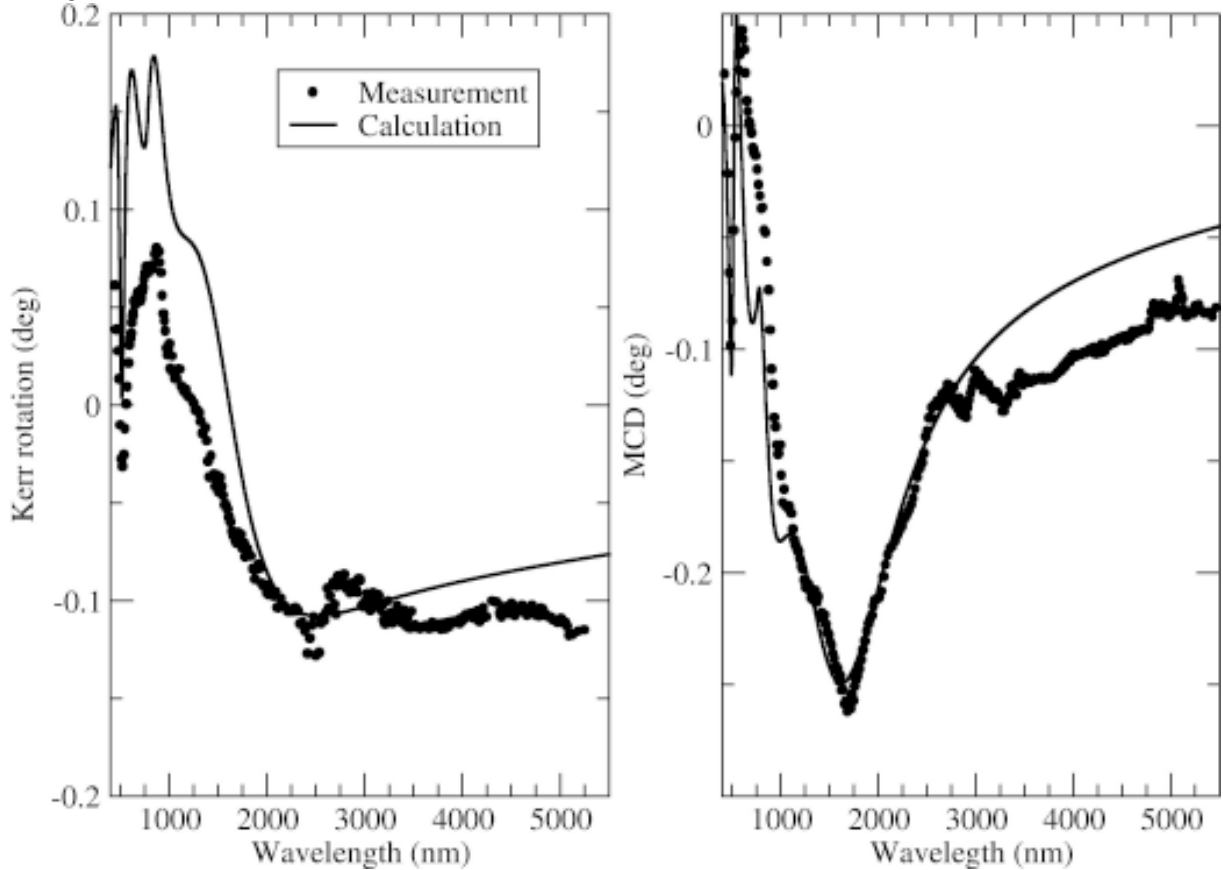


Fig. 9. Kerr and MCD spectra for InMnAs ($x=0.08$) at a fixed magnetic field of 4.5 kG and temperature $T=1.6$ K.

where a maximum is observed, a σ^- (left circularly polarized) transition is resonant with the photon energy; while a minimum corresponds to a σ^+ transition. By this method one can experimentally determine transition energies for different magnetic fields. Fig. 7 demonstrates an excellent agreement between these data and model calculations.

Fig. 8 shows measured Kerr rotation and MCD spectra of InMnSb and theoretical spectra calculated with $N_0\alpha=2.16$ eV and $N_0\beta=3.1$ eV. The oscillations are interference fringes due to the multilayer sample. In the theoretical spectra the multiple reflections are calculated using the transfer matrix method [11]. The exchange parameters resulting from the fit to the experimental Kerr and MCD spectra are extraordinarily high compared to II-VI materials as well as to GaMnAs [4]. Further investigations are necessary to check these values and to find the reason for the extremely high values obtained in the present case. A reasonable explanation is based on the density of states calculations using LDA (local density approximation) published in Ref. 12 for InMnAs: Additional circularly polarized interband transitions may arise from the hybridization of spin-split delocalized 3d-electrons with holes near the Fermi-level in the valence band. The electric dipole moment couples these d-states strongly with the conduction band electrons which possess a considerable p-admixture due to the strong non-parabolicity in narrow-gap semiconductors.

Fig. 9 shows the spectra observed for InMnAs. In this case the fits yield the values $N_0\alpha=0.3$ eV and $N_0\beta=1.5$ eV. These values are of the same order of magnitude as found in other DMSs with Mn. At short wavelengths there are sharp minima due to transitions at the L-point which are not covered by the theory, and are therefore included heuristically. Inadequacy of this description is responsible for the relatively large difference between experi-

ment and calculation in the Kerr rotation spectrum for wavelengths shorter than 1000 nm.

6. SUMMARY

Magneto-optical experiments are very well suited for investigating diluted magnetic semiconductors, particularly those which exhibit long range ferromagnetic order. Complex theories have to be used to describe these effects in narrow gap semiconductors such as InMnSb, since the non magnetic hosts of those materials exhibit large spin splittings that may be comparable in magnitude to the effects caused by the magnetic interaction with the incorporated Mn ions.

REFERENCES

- [1] H.-R. Trebin *et al.* // *Phys. Rev. B* **20** (1979) 686.
- [2] J. Schmitz *et al.* // *Computer Physics Communications* **66** (1991) 308.
- [3] C. Rigaux, In: *Semiconductors and Semimetals*, Vol. **25**, ed. by J. K. Furdyna and J. Kossut (Academic, Boston, 1988), p. 229.
- [4] R. Lang *et al.* // *Phys. Rev. B* **72** (2005) 024430-1.
- [5] H. Ohno *et al.* // *Appl. Phys. Lett.* **69** (1996) 363.
- [6] T. Dietl // *Semicond. Sci. Technol.* **17** (2002) 377.
- [7] T. Wojtowicz *et al.* // *Appl. Phys. Lett.* **82** (2003) 4310.
- [8] H. Munekata *et al.* // *Appl. Phys. Lett.* **63** (1993) 2929.
- [9] J.K. Furdyna // *J. Appl. Phys.* **64** (1988) R29.
- [10] C. Kim *et al.* // *Phys. Rev. B* **45** (1992) 11749.
- [11] P. Yeh // *Surf. Sci.* **96** (1980) 41.
- [12] H. Akai // *Phys. Rev. Lett* **81** (1998) 3002.